THE ROYAL SOCIETY

doi 10.1098/rspb.2000.1415

Geometrical and crystallographic constraints determine the self-organization of shell microstructures in Unionidae (Bivalvia: Mollusca)

Antonio G. Checa[1]* **and Alejandro Rodríguez-Navarro**[2]

[1]*Departamento de Paleontología y Estratigrafía, Universidad de Granada, Granada 18002, Spain*
[2]*Savannah River Ecology Laboratory, University of Georgia, Drawer E, Aiken, SC 29802, USA*

Unionid shells are characterized by an outer aragonitic prismatic layer and an inner nacreous layer. The prisms of the outer shell layer are composed of single-crystal fibres radiating from spheruliths. During prism development, fibres progressively recline to the growth front. There is competition between prisms, leading to the selection of bigger, evenly sized prisms. A new model explains this competition process between prisms, using fibres as elementary units of competition. Scanning electron microscopy and X-ray texture analysis show that, during prism growth, fibres become progressively orientated with their three crystallographic axes aligned, which results from geometric constraints and space limitations. Interestingly, transition to the nacreous layer does not occur until a high degree of orientation of fibres is attained. There is no selection of crystal orientation in the nacreous layer and, as a result, the preferential orientation of crystals deteriorates. Deterioration of crystal orientation is most probably due to accumulation of errors as the epitaxial growth is suppressed by thick or continuous organic coats on some nacre crystals. In conclusion, the microstructural arrangement of the unionid shell is, to a large extent, self-organized with the main constraints being crystallographic and geometrical laws.

Keywords: biomineralization; bivalve shell; microstructure; nacre; composite prisms; self-organization

1. INTRODUCTION

Molluscs fabricate shells that are composites of calcite or aragonite crystals embedded within an organic matrix. The crystals display varied morphologies and structural arrangements and are described as having different microstructures. In most cases, the shells are constructed of two or more superimposed layers with different microstructures, which may even be composed of different calcium carbonate polymorphs (i.e. calcite or aragonite) (Taylor *et al.* 1969).

Shell formation starts with the secretion of an outer organic membrane or periostracum (figure 1). This organic membrane acts as the substrate where shell-forming crystals (calcium carbonate in either the form of calcite or aragonite) nucleate. The shell-secreting epithelium or mantle supplies the Ca^{2+} and HCO_3^- ions necessary for the growth of calcium carbonate crystals. The mantle is separated from the inner shell surface by a space. The organism can maintain a supersaturated solution (extrapallial fluid) within this space, thereby allowing shell-forming crystals to precipitate (Simkiss & Wilbur 1989). There is evidence from *in vitro* experiments that specific proteins composing the shell organic matrix play an important role in controlling the polymorphic phase, morphology and orientation of individual crystals (Addadi *et al.* 1987; Falini *et al.* 1995; Belcher *et al.* 1996). However, little is known about the role these proteins play in how crystals assemble into a given microstructure. Since different species have specific shell microstructures it is generally believed to be genetically directed (Addadi & Weiner 1992). Even more striking is the transition between superimposed layers with different microstructures. For instance, in Unionidae the mantle secretes two shell layers with different microstructures. The mantle has an oblique disposition with respect to the periostracum, depositing the two different layers simultaneously (figure 1). The more marginal areas of the mantle secrete the outer shell layers. This is usually explained by assuming a zonation of the metabolic properties of the shell-secreting mantle surface (Beedham 1958). In this way, different parts of the mantle could induce the development of different microstructures.

While understanding biomineralization processes has been the main focus of studying shell growth, the knowledge may also be applied to the fabrication of superior materials composed of highly orientated crystals of the same size and morphologies (Aksay *et al.* 1996). For instance, the structure of mollusc shell, in particular nacre (which is formed by layers of aragonite tablets sandwiched by an organic membrane), has excellent mechanical strength and fracture toughness, exceeding that of the aragonite single crystals composing it by several orders of magnitude (Currey 1977).

Most studies on mollusc shell growth have focused on the physiological factors controlling shell growth (Saleuddin & Kunigelis, 1984; Simkiss & Wilbur 1989; Addadi & Weiner 1992) and the role of specific proteins in the control of crystal growth (Lowenstam & Weiner 1989). However, much less attention has been paid to fundamental issues such as the geometrical and crystallographic factors constraining the growth of crystals and the development of aggregate micro-architectures. For instance, simple geometrical laws govern the growth of crystals. Crystal habit depends entirely upon the relative growth rates of crystal faces, which are in turn controlled by both crystal structure and growth conditions (i.e. supersaturation, temperature and impurities (proteins))

*Author for correspondence (acheca@ugr.es).

Received 10 November 2000 *Accepted* 5 December 2000

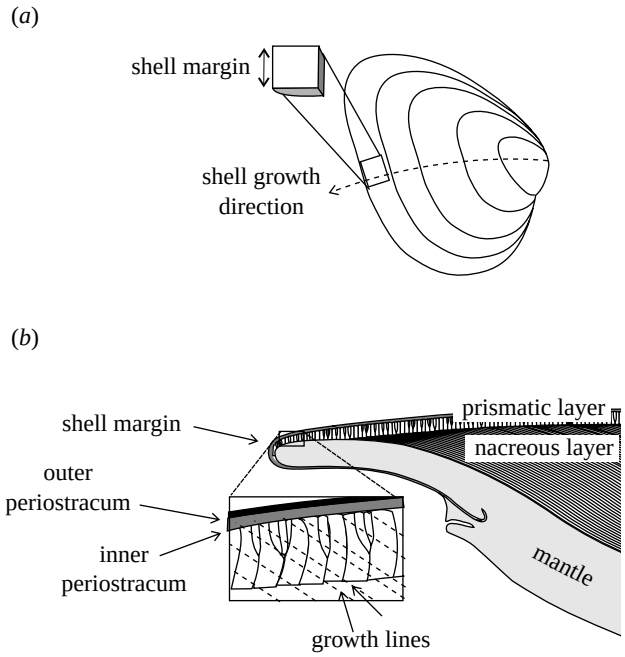

Figure 1. (*a*) Drawing of a unionid shell with the main reference directions indicated and showing where shell pieces were cut for the texture analysis. (*b*) Schematic of a cross-section of a shell showing the disposition of the different layers constructing it. Modified from Checa (2000).

(Sunagawa 1987). The growth of a polycrystalline aggregate (i.e. shell) is much more complex as crystals growing together impinge on each other and compete for the available space, but its growth is still governed by crystallographic and geometrical laws (Grigor'ev 1965; Rodríguez-Navarro & García-Ruiz 2000). In this paper, we focus on the evolution of the morphology and crystallographic orientation of crystals during shell growth in unionids in order to evaluate the importance of geometrical and crystallographic factors versus biological factors on the development of shell micro-architectures.

2. MATERIAL AND METHODS

(a) *Material*

Shells of the Unionidae were studied including *Unio elongatulus* Pfeiffer, 1825, (Canal Imperial de Aragón, Navarra, Spain), *Unio crassus* Philippson, 1788 (River Meuse, Hastières, Belgium), Ambleminae *Potomida littoralis* (Lamarck, 1801) (Canal Imperial de Aragón, Zaragoza, Spain), *Lamprotula* sp. (locality unknown, China) and *Caelatura bakeri* (Adams, 1866) (Nyanza, Kenya).

(b) *Optical and electron microscopy*

Thin sections (30–40 µm thick) of *U. elongatulus* and *Lamprotula* sp. shells cut along a dorsoventral radius were prepared for transmitted light microscopy. The mantle shell system was studied in living specimens of *U. elongatulus* and *P. littoralis*. Samples were initially fixed in 10% formalin and preserved in 70% ethanol. Square pieces of the shell margin (usually the ventral area) were cut very carefully in order to avoid damaging the adjacent mantle margin. The mantle was later cut with precision scissors. The samples were later completely decalcified, fixed in buffered cacodylate (0.1 M and pH 7.4) 2.5% glutaraldehyde and critical point–CO_2 dried. They were later embedded in epoxy resin, sectioned to 1 µm (Ultracut S, Leica, Solms, Germany) and stained with 1% toluidine blue. Samples were superficially decalcified with 6% ethylenediaminetetraacetic acid for 20 min at room temperature for scanning electron microscope (SEM) examination. Outer and inner valve surfaces (sometimes with the periostracum partly removed with 5% NaOH) as well as transverse radial fractures of shells (intact or etched in 1% HCl for less than 1 min) from all species (except *P. littoralis*) were observed in an SEM (DSM 950, Zeiss, Jena, Germany) after being sputtered with gold for 4 min.

(c) *X-ray texture analysis*

The orientation of the crystals of *U. elongatulus* and *Lamprotula* shells was determined using an X-ray texture diffractometer (X'pert, Phillips, Amelo, The Netherlands) (Cullity 1977). Pole densities for 002 and 112 reflections of aragonite were registered in order to do this. These pole figures show the three-dimensional distribution of orientation of the [001] and [112] crystal directions. The stereographic projections of the pole figures are displayed as counter plots. The scattering or degree of preferential orientation of crystals can also be quantified from these plots as full width at half maximum (FWHM) values of the peaks in the pole figures. The lower the FWHM value, the greater the alignment of crystals. In order to study the evolution of the orientation of crystals during shell growth, samples were manually ground to different levels parallel to the outer shell surface and the pole figures registered.

3. RESULTS

(a) *The internal structure of prisms*

Unionid shells consist of an outer aragonitic prismatic layer and an inner nacreous layer with the prismatic layer comprising only *ca.* 10% of the total shell thickness. Shell growth occurs via spheruliths (spherical aggregates of radiating crystal fibres) that nucleate within the gelatinous

inner periostracal surface (figure 2*a*,*g*). Initially, spheruliths grow independently from each other but, as growth continues beyond the boundary of the inner periostracum, they start to impinge on one another and develop into polygonal prisms. Prisms grow vertically (inward) and later they usually become gradually reclined towards the shell margin (figure 2*b*). In this way, the prism main axis remains perpendicular to the growth front (see below). Its orientation changes gradually from being inclined dorsal-wards to nearly parallel to the periostracum at the very margin. Prisms are composed of elongate crystals (fibres) fanning out in three dimensions from the main axis of the prism towards the depositional surface. Longitudinally fractured prisms, as observed through the SEM, show particularly conspicuous fibres towards the edges of prisms (figure 2*c*,*f*). During prism growth, fibres fan out (giving the prisms a feather-like appearance in cross-section) (figure 2*b*,*e*) and become thicker, reaching up to 2 µm in thickness at their most distal ends (figure 2*c*). Each fibre is a single, curved crystal with the *c*-axis parallel to the long axis as revealed by the undulating extinction pattern with polarized light microscopy (figure 2*b*). As prisms grow longer, the mean divergence of fibres with the main or long axis of the prisms decreases. Values of 20–25° at the lower boundary of the prismatic layer are typical. At the same time, fibres achieve greater lengths and become straighter (figure 2*b*,*c*). The distribution of fibres within a prism is asymmetric. Fibres running forwards (pointing to the shell margin) grow more than those diverging backwards (figure 2*c*). In this way, while fibres remain strictly perpendicular to the growth front, the prism long axis becomes progressively advanced with respect to the axis of fibre divergence and the shell margin. Prisms show prominent concentric growth lines (figure 2*a*,*e*) that are more or less centred in the spheruliths. They are perpendicular to the fibres and remain as organic sheets after decalcification. These growth surfaces most probably reflect successive positions of the mantle. Interestingly, the deposition of these organic sheets does not seem to interrupt or alter fibre growth and orientation.

(b) *The size and shape of prisms*

During growth of the prismatic layer, bigger prisms expand laterally at the expense of smaller ones, thereby blocking their space for growing. Prismatic units are progressively lost so that only a few, big, evenly sized prisms reach the transition to the nacreous layer (figure 2*a*,*e*,*f*). The thickness of the prismatic layer as well as the size of the prisms (both in height and width) increases in a radial section from older to newer parts of the shell (i.e. the shell margin). The spacing among neighbouring prisms also increases in the same direction.

The variation in the aspect ratio (height to width) of prisms is shown in figure 3 as a function of their height. It can be observed that prisms show a trend of increasing elongation (higher aspect ratios) with increasing height. However, there is a tendency for the value of the aspect ratio to saturate as the prisms' size (height) increases further. Furthermore, as the aspect ratio of the prisms increases, the limit angle or maximum angle of divergence of fibres decreases.

(c) *Transition to the nacreous layer*

Large distal fibres of the surviving prisms become transversely divided by organic sheets at the transition zone from the prismatic to the nacreous layer and gradually transform into stacked nacreous tablets (figure 2*c*). Fibres are highly aligned (within a range of 20°) at the transition zone. The first nacreous tablets grow epitaxially onto the distal ends of fibres, from which they inherit their crystallographic orientation, having their *c*-axis perpendicular to the tablet surface. The transition to nacre is initiated in the rear part of a radial section of a shell within individual prisms and proceeds to the front part of the prism that is pointing towards the shell margin (figure 2*c*). The first nacre sheets usually have a slightly wavy disposition that results from the diverging arrangement of fibres. Waviness soon fades out and the nacre sheets become flat as the nacreous layer grows thicker. Similar gradual transformations were observed by Dauphin *et al.* (1989) in *Haliotis* and Mutvei (1972) in *Nautilus*.

(d) *The inner surface of the shell*

The inner surface of the inner nacreous layer shows a terraced disposition of the aragonite sheets, which grow towards the shell margin (figure 2*d*). Sequential stages of the nacreous tablet nucleation and growth can be observed when moving towards the shell edge. The shape of aragonite tablets is rhombic, with the longest diagonal coincident with the *b*-axis and the shortest coincident with the *a*-axis. The elongate crystal shape reflects a faster growth rate along the *b*-axis than the *a*-axis. Note that crystals forming a nacre lamella or sheet are orientated with their longest diagonal (*b*-axis) towards the direction of shell growth and the shorter diagonal (*a*-axis) transversal to it and parallel to the shell margin. However, exceptions are sometimes noted in isolated tablets or even clusters of tablets with orientation differing significantly from the common orientation (*b*-axis perpendicular to the shell edge), sometimes even being transverse (figure 2*d*).

(e) *Evolution of the orientation of crystals during shell growth*

The evolution of the orientation of crystals during shell growth was studied by registering pole figures at different thickness within a shell of *U. elongatulus*. The pole figures from the outer surface of the shell (thickness 0%), which correspond to the initial stages of shell formation, show a uniform distribution of intensity indicating that crystals nucleate with a random orientation. At increasing thickness, corresponding to later stages of growth, the pole figures gradually show better-defined peaks, indicating that crystals are progressively more aligned (figure 4). The degree of alignment of crystals is assessed by the FWHM value for these peaks (figure 4). The FWHM χ-value in figure 4*c* (left-hand graph), which was measured from the 002 pole figures, decreases rapidly across the prismatic layer, reaching a minimum just after the transition to the nacreous layer. It increases again across the nacreous layer indicating that the scattering of the orientation of the *c*-axis of crystals follows the same trend. Curiously, the scattering of the *c*-axis is greater in the direction parallel to than the direction perpendicular to the shell margin. The spread of the orientation of the

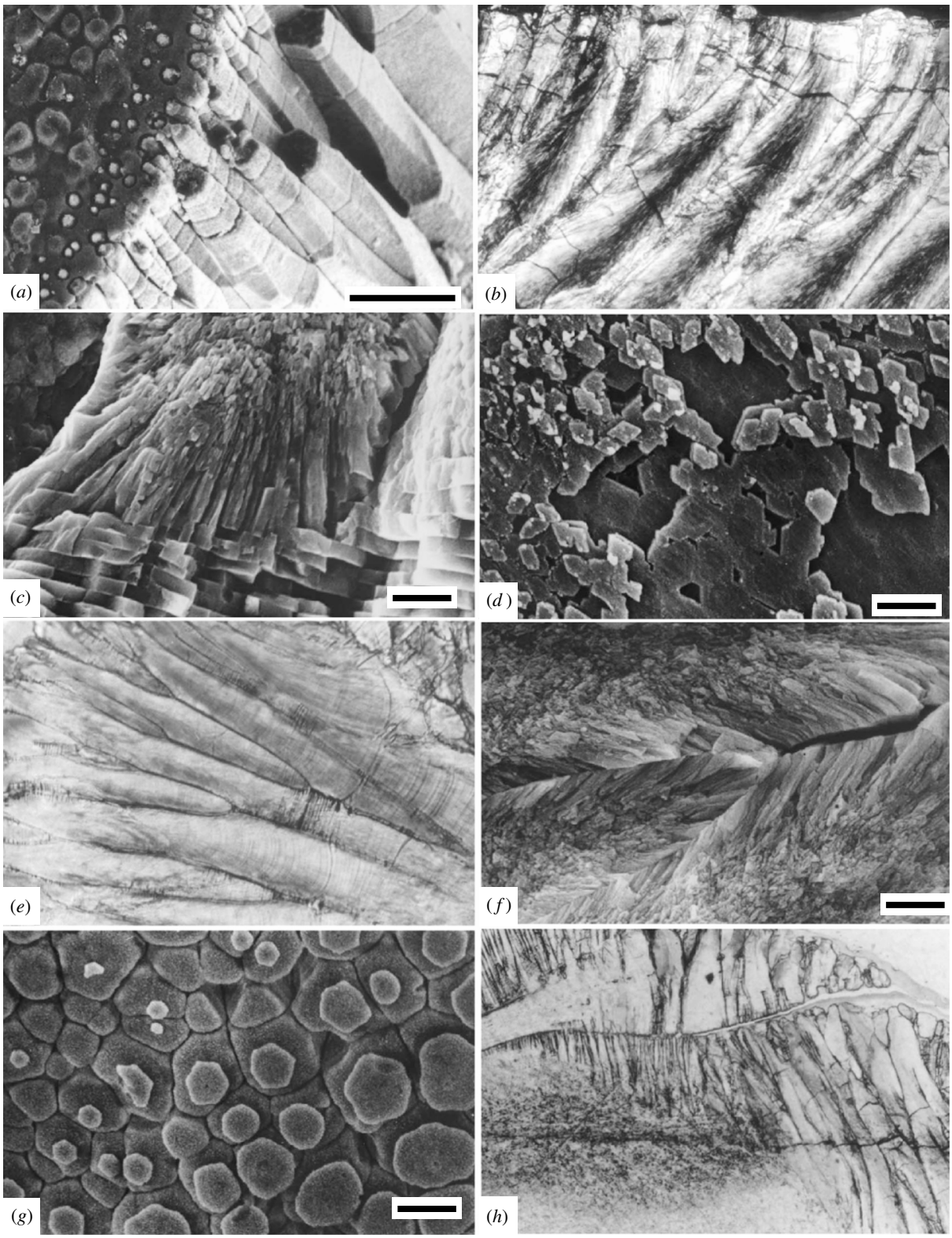

Figure 2. (*Caption opposite.*)

a- and *b*-axes, which was measured as the FWHM ϕ-value from peaks of 112 pole figures, follows the same trend as that of the *c*-axis (figure 4*c*, right-hand graph), though the alignment of crystals along these axes is always poorer than along the *c*-axis. These observations imply that crystals that initiate shell growth are randomly orientated. Crystals become rapidly aligned during the growth of the prismatic layer. However, their orientation deteriorates slightly during the growth of the nacreous layer.

Intraprismatic growth lines, which are formed by organic material, cross cut the different prisms indicating pulsating growth of the whole layer (figure 2*a*,*e*). Interestingly, the deposition of organic material does not seem to interrupt the epitaxial growth of crystals from one layer to the next. In fact, SEM and X-ray texture analysis shows that, during shell growth, there is always continuity in the preferential orientation of crystals and that only the degree of alignment changes.

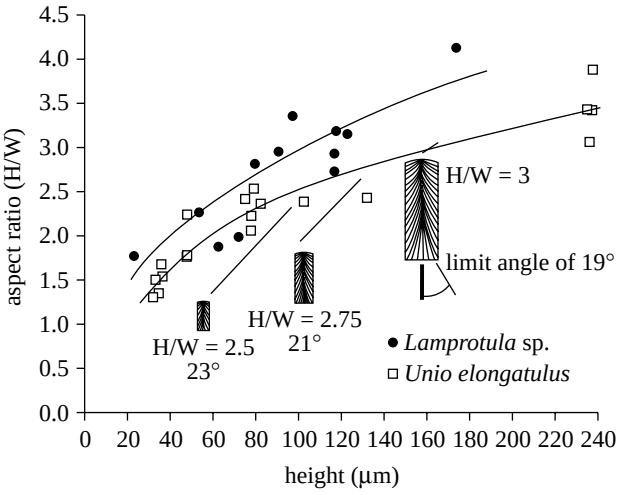

Figure 3. Aspect ratio (height to width (H/W)) of prisms as a function of their size (height) measured for Unionidae shells. Values were obtained from SEM views of sections either parallel (*U. elongatulus*) or transversal (*Lamprotula* sp.) to the margin. Prisms become more elongate with size.

4. DISCUSSION

(a) *Competition between prisms*

Competition between prisms was described and interpreted by Ubukata (1994) in several bivalves, including unionids. He developed geometrical constructions based on Grigor'ev's (1965) model of the growth of aggregate minerals in order to show the effect of several factors on prism selection. The main problem when these models are applied to the composite prisms of unionids is that they imply a free-growing surface (as in the formation of, for example, quartz crystals growing on the wall of a rock cavity or geode). However, in unionids the mantle surface limits prism growth, as evidenced by growth lines. Therefore, unlike Grigor'ev's (1965) model, the growth front of prisms is permanently constrained by the position of the mantle, thereby precluding the possibility of differences in the longitudinal growth rate among prisms. Taking this into consideration, we have developed a model in which prism selection is not due to competition between prisms, but between the fibres of different prisms meeting at the interprismatic surfaces (figure 5). When a prism outcompetes another it is apparent that its fibres run less inclined to the growth front (figure 2*f*). A lesser inclination angle implies a faster growth in parallel to the growth surface, which explains why less-inclined fibres outcompete more-inclined ones. Therefore, competition between prisms can be reduced to competition between their constituent fibres. A growth rate normal to the growth surface is a negligible factor since fibre growth in this direction is constrained by the rate of mantle displacement, which is uniform for fibres of all prisms growing at the same time.

(b) *Genesis and evolution of crystal orientation*

It has been suggested that crystal orientation is imposed by epitaxial nucleation on the organic matrix surface (Weiner & Traub 1980, 1984). However, the degree of orientation of the organic constituents and the range over which they are orientated (a few microns) are

Figure 2. (*a*) Oblique view of a partly dissolved inner periostracum and fractured outer prismatic layer of *Lamprotula* sp. Growth surfaces cross cut adjacent prisms. Growth direction, top left to bottom right. Magnification × 420. (*b*) Polarized light micrograph of the outer prismatic layer of *U. elongatulus*. Prisms are composed of fibres diverging from the prism main axis. Extinction bands usually displace rearwards (right) during prism growth (to the bottom) indicating that fibres directed forwards to the shell margin become progressively more developed at the expense of those directed backwards. Prisms curve to remain perpendicular to the growth front. Magnification × 190. (*c*) Transition between the prismatic and nacreous layers in *Lamprotula* sp. Prism-composing fibres gradually align parallel to the long axis of the prism. Transition to the nacreous layer occurs when the degree of convergence reaches a certain threshold. Fibre distribution is asymmetric with those running forwards to the shell margin (right) being more developed. This causes transition to the nacreous layer to proceed from the rear of the prism forwards. Magnification × 1800. (*d*) View of the step-like arrangement of nacreous sheets at the internal growth surface of the shell of *P. littoralis*. Rhombic nacreous tablets are orientated, with minor exceptions, with their longest diagonal (*b*-axis) parallel to the shell growth direction (upper left). Magnification × 1800. (*e*) Thin section through the outer prismatic layer of *P. littoralis*. Intraprismatic growth surfaces are perpendicular to fibres and, hence, concave towards the initial spherulith. They continue across the different prisms, which indicates synchronized growth. Magnification × 190. (*f*) Prismatic shell of *Lamprotula* sp. Two prisms outcompete a third trapped in-between. When fibres meet, those of the bigger prisms always form a higher angle with the long axes of prisms. Magnification × 1800. (*g*) Outer shell surface of *Lamprotula* sp. with the periostracum removed. Initial spheruliths are statistically placed towards the rear of prisms (lower right), which indicates an asymmetric development of prisms. Magnification × 850. (*h*) Section through the prismatic and nacreous layers of *U. elongatulus*. Growth halts are marked by discontinuities. Growth resumes with prismatic layers that intrude into the nacreous layer and gradually wedge out internally. Prism size decreases in the same direction, so that the relationship of width to height is kept. Magnification × 95. Scale bars: (*a*) 50 μm, (*c*,*d*,*f*) 5 μm and (*g*) 10 μm.

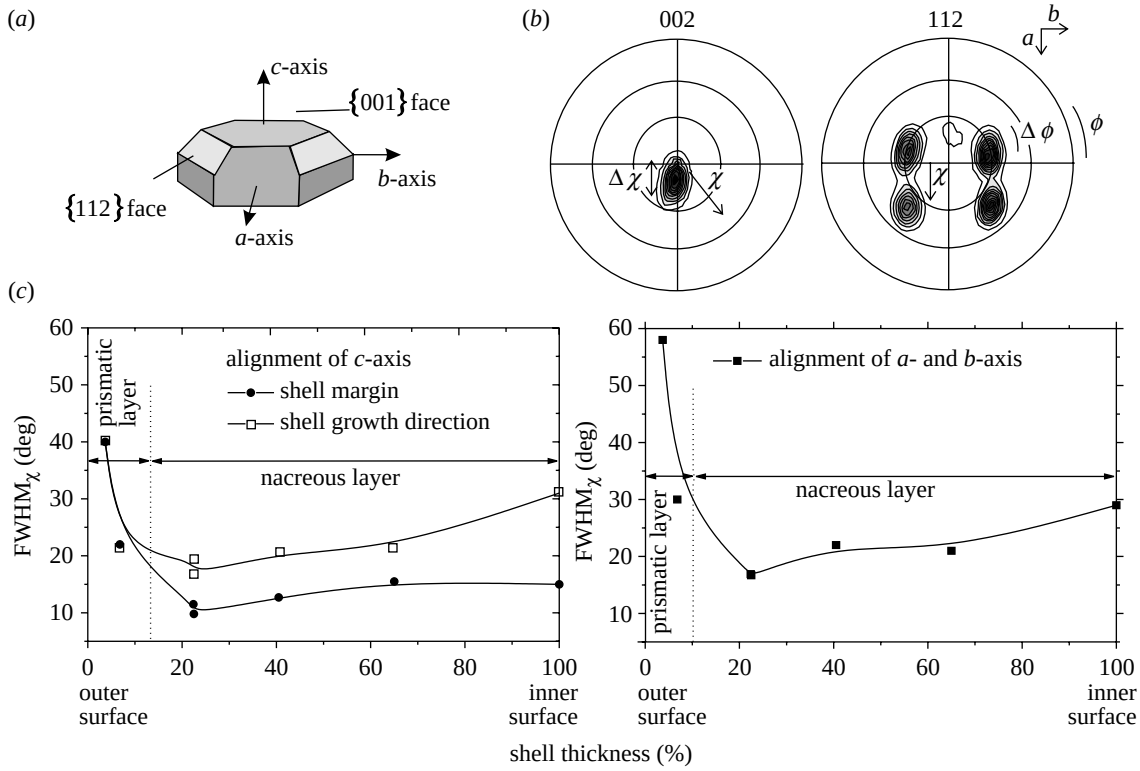

Figure 4. (*a*) Single crystal of aragonite. (*b*) Distribution of crystal orientations measured at the boundary between the prismatic and nacreous layers. The subcentral position of unique maxima in the 002 pole figure indicates that the crystals are orientated with their *c*-axis perpendicular to the shell surface. The positions of the four maxima displayed in the 112 pole figure indicate that the crystals orientate with their *b*-axes parallel to the shell growth direction (horizontal line) and *a*-axes parallel to the margin. (*c*) Evolution of the alignment of crystals across the shell thickness (left-hand graph) along the *c*-axis and (right-hand graph) along the *a*- and *b*-axes. Interestingly, the crystals become aligned within the prismatic layer (FWHM values decrease), whereas their alignment deteriorates as the nacreous layer becomes thicker (FWHM values increase).

much less than those of aragonite crystals (in the order of millimetres) (Weiner & Traub 1984). In addition, such a mechanism does not explain the evolution of the orientation of crystals during shell growth and, contrary to observation, it implies that the orientation of crystals is already selected in early crystal growth stages. Conversely, we observed that preferential orientation of crystals in the shells of unionids develops during growth of the prismatic layer, starting from randomly orientated crystals.

This progressive alignment of crystals during prism growth is due to geometric selection of crystals. The progressive alignment of fibres and the *c*-axis of crystals with the main axis of the prisms is merely a geometric feature. Initially, fibres of the spheruliths (from which prisms initiate) radiate in all directions. As growth progresses these fibres impinge on fibres of neighbouring spheruliths, thereby constraining further growth of fibres to the sides. Fibres only have free space for developing vertically. As the prismatic layer becomes thicker the orientation of fibres is further selected and only fibres orientated vertically (growing inward) continue to grow (figure 6). Sylin-Robert (1986) described a similar model in explaining the development of a preferential orientation of crystals in eggshells along their *c*-axis. However, in order to explain the orientation of crystals with their *a*–*b*-axis also aligned another mechanism must be invoked. The horizontal displacement of the mantle at the shell margin frees some space for the expansion of fibres in the *a*–*b*-plane towards the shell margin. This allows geometrical selection of fibres orientated with their horizontal, fastest, growth direction (*b*-axis) perpendicular to the shell margin (figure 6). This process results in the crystal fibres having their three axes aligned. However, the degree of alignment of crystals along the *a*–*b*-axes is less than that along the *c*-axis. The selection mechanism is more efficient along the *c*-axis since the orientation of crystals is due to differences in growth rates along different crystal directions and the *c*-axis is the overall faster crystal growth direction.

(c) *Transition to the nacreous layer*

Interestingly, the transition to nacre does not occur until the angular divergence of fibres (and that of *c*-axes) within prisms falls below a certain threshold (within *ca.* 20°). It seems as if a uniformly orientated substrate (or at least one with a reduced range of dispersion) is necessary for nacre to grow by epitaxy. This is not surprising since a main characteristic of nacre is that the tablets have their *c*-axis aligned and orientated perpendicular to the shell surface (e.g. Hedegaard & Wenk 1998). It is probably not accidental that molluscan nacre is, in most cases, preceded by some kind of fibrous or prismatic (either aragonitic or calcitic) layer (Taylor *et al.* 1969).

Since fibres curve outwards, bigger prisms will attain the *c*-axis dispersal threshold relatively late and could grow longer (higher aspect ratios) (figures 2*h* and 3).

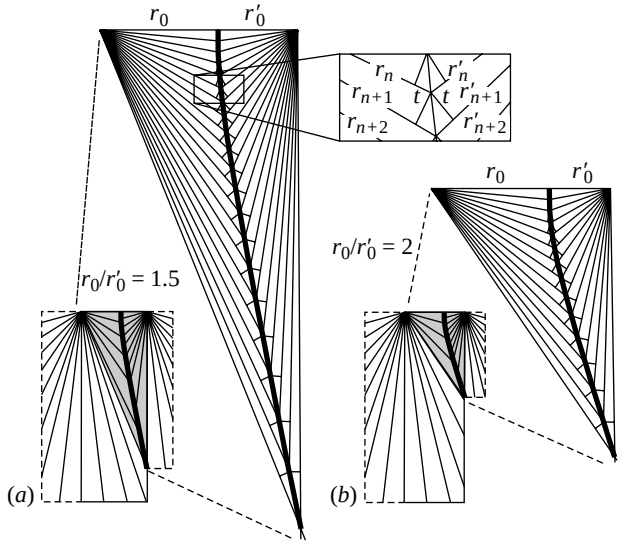

Figure 5. Model for competition between composite prisms in Unionidae. When two fibres (r_n and r'_n) meet, the subsequent pair of impinging (r_{n+1} and r_{n+1}') can be obtained at fixed distances (t) measured from their ends, perpendicular to the radii. When two prisms of different size collide, the fibres of the bigger prism always meet those of the smaller prism at a lesser angle to the horizontal (growth front). Displacement is faster as the difference in width between prisms (r_0/r'_0) is greater. Two examples are provided for comparison. (*a*) $r_0/r'_0 = 1.5$ and (*b*) $r_0/r'_0 = 2$.

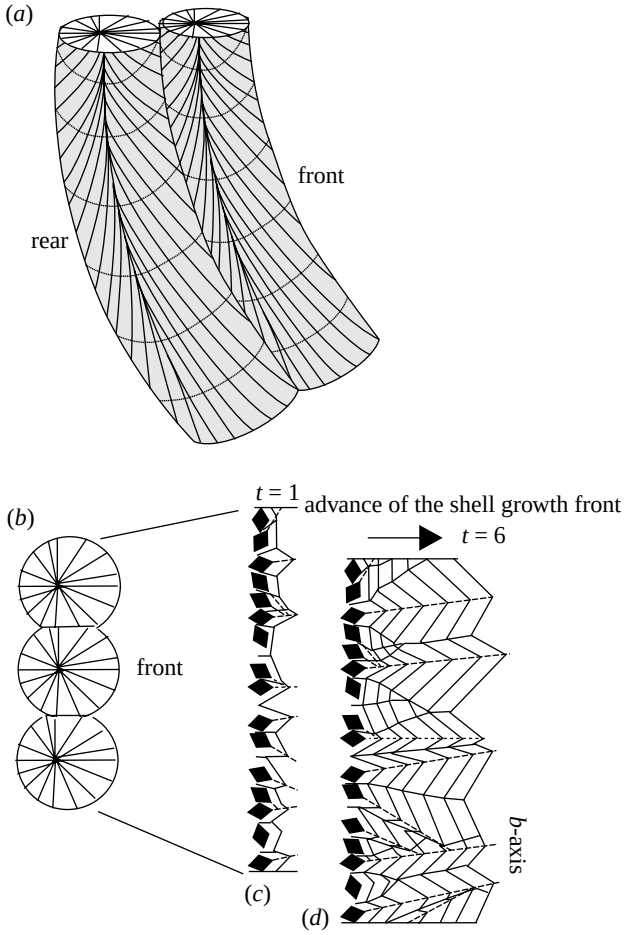

Figure 6. Competitive growth model for the alignment of *a*- and *b*-axes of fibres during prism growth. (*a*) Sketch of a longitudinal section of prisms parallel to the shell growth direction of the shell margin (right). See also figure 1*g*. Prisms initiate as asymmetric spheruliths, with a more developed frontal part, towards the shell margin. This causes the rear prism to displace the one in front of it progressively, while, in turn, it is displaced by the prism behind (not shown). As a consequence, the fibres running in a frontal direction become progressively more developed. (*b*) View of prisms parallel to the shell surface. (*c*,*d*) As fibres grow longer and thicker, competition in the *a*–*b* plane (cross-section of fibres) causes selection of those fibres having their fastest horizontal growth direction (*b*-axis) orientated parallel to the shell growth direction (arrow).

More remarkable is the fact that the transition to nacre occurs in the rear part of the prism first rather than in the front part of the prism (figure 2*c*). The asymmetrical distribution of fibres within prisms causes the *c*-axis dispersal threshold to be reached first at the back, with the subsequent secretion of the first nacreous tablets, and to propagate forward later. The asymmetric development of prisms can be traced back to the initial spherulith stage. Spheruliths are usually more developed anteriorly since growing spheruliths have more free space to expand forwards than backwards where older spheruliths are already expanding (figure 2*g*).

Nacreous tablets inherit the crystallographic orientation of the most distal fibres of prisms, which act as epitaxial mineral substrates. As the nacreous layer grows thicker the orientation of crystals deteriorates, as revealed by X-ray texture analysis and through the SEM (see above) (figure 4). In our opinion, this is probably due to two factors. First, the orientation of crystals is not further selected by competition since crystals nucleate separately and only establish contact when fully grown (figure 2*d*). Second, there may be an accumulation of errors in which the epitaxial growth of crystals from one nacre sheet to the next is suppressed. There are porous organic coats between nacre sheets that allow physical contact and, hence, epitaxy between crystals of different layers (Schaffer *et al.* 1997). However, a thick or continuous organic coat could prevent epitaxial growth and cause the new crysal to have a random orientation (figure 7).

Finally, in our opinion, genetic factors must determine the shape of the mantle and periostracum, which define the geometry of the cavity where shell mineralization occurs. In addition, cellular processes might be responsible for the secretion of specific organic components (i.e. proteins), which must certainly modulate the crystal growth. However, it should be noted that, once crystal growth is initiated, the subsequent arrangement of crystals is mostly determined by crystallographic constraints and space limitations, with the resulting aggregate microstructure being self-organized.

5. CONCLUSIONS

The microstructural development of the shell in Unionidae can be understood when the monocrystalline fibres (instead of prisms, into which they aggregate) of the outer shell layer are considered as elementary units. In particular, we have explained (i) competition and selection between prisms, (ii) the development of the orientation of

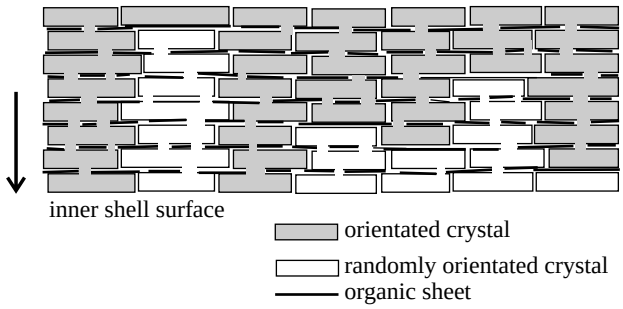

Figure 7. Model of accumulation of defects within the nacreous layer. Tablets of a new nacre sheet will grow epitaxially on the previous sheet, provided that pores of the organic sheet allow them to establish direct contact. Otherwise, new tablets will nucleate with random orientation. These defects accumulate since new nacre tablets can nucleate epitaxially on randomly orientated crystals.

crystal fibres within the prismatic layer starting from spheruliths, (iii) the transition from the prismatic to the nacreous layer, and (iv) increasing scattering of crystal orientation with addition of new nacreous sheets, as mere geometrical and crystallographic processes. These processes are regarded as epiphenomena arising from the anisotropic growth rates of biogenic aragonite crystals. In summary, the inner periostracum serves as the substrate for nucleation of spheruliths, whereas the mantle supplies calcium carbonate and organic components to the shell growth front via the extrapallial space. Finally, our observations suggest that the physical factors determining the self-organization of shell microstructures deserve as much attention as genetic ones in explaining the formation of the bivalve shell.

This study was financed by research project PB97-0790 of the Dirección General de Enseñanza Superior e Investigación Científica (Ministerio de Educacion y Ciencia, MEC), research group RNM-0178 (PAI, Junta de Andalucía) and an award (DE-FC09-96-SR18546) from the US Department of Energy to the University of Georgia Savannah River Ecology Laboratory. We also thank the postdoctoral program of the MEC (Spain). We are very grateful to Professor Chris Romanek (Savannah River Ecology Laboratory), Robert C. Thomas (Savannah River Ecology Laboratory) and Professor Russell Messier (Penn State University) for their useful comments and support.

REFERENCES

Addadi, L. & Weiner, S. 1992 Control and design principles in biological mineralization. *Angew. Chem. Int. Ed. Engl.* **31**, 153–169.

Addadi, L., Moradian, J., Shay, E., Maroudas, N. G. & Weiner, S. 1987 A chemical model for the cooperation of sulfates and carboxylates in calcite crystals formation. *Proc. Natl Acad. Sci. USA* **84**, 2732–2736.

Aksay, I. A., Trau, M., Manne, S., Honma, I., Yao, N., Zhou, L., Fenter, P., Eisenberger, P. M. & Gruner, S. M. 1996 Biomimetic pathways for assembling inorganic thin films. *Science* **273**, 892–898.

Beedham, G. E. 1958 Observations of the mantle of the Lamellibranchia. *Q. J. Microscopial Sci*.

Belcher, A. M., Wu, X. H., Christensen, R. J., Hansma, P. K., Stucky, G. D. & Morse, D. E. 1996 Control of crystal phase switching and orientation by soluble mollusc-shell proteins. *Nature* **381**, 56–58.

Checa, A. 2000 A new model for periostracum and shell formation in Unionidae (Bivalvia, Mollusca). *Tissue Cell*. (In the press.)

Cullity, B. D. 1977 *Elements of X-ray diffraction*, 2nd edn, pp. 127–131. Reading, MA: Addison-Wesley.

Currey, J. D. 1977 Mechanical properties of mother of pearl in tension. *Proc. R. Soc. Lond.* B **196**, 443–463.

Dauphin, Y., Cuif, J. P., Mutvei, H. & Denis, A. 1989 Mineralogy, chemistry and ultrastructure of the external shell-layer in ten species of *Haliotis* with reference to *Haliotis tuberculata* (Mollusca: Archaeogastropoda). *Bull. Geol. Inst. Univ. Uppsala* **15**, 7–38.

Falini, G., Albeck, S., Weiner, S. & Addadi, L. 1995 Control of aragonite or calcite polymorphism by mollusk shell macromolecules. *Science* **271**, 67–69.

Grigor'ev, D. P. 1965 *Ontogeny of minerals*. Jerusalem: Israel Program for Scientific Translations.

Hedegaard, C. & Wenk, H.-R. 1998 Microarchitecture and texture patterns of mollusc shells. *J. Moll. Stud.* **64**, 133–136.

Lowenstam, H. A. & & Weiner, S. 1989 *On biomineralization*. New York: Oxford University Press.

Mutvei, H. 1972 Ultrastructural relationships between the prismatic and nacreous layers in *Nautilus*. *Biomineral. Res. Rep.* **4**, 81–86.

Rodríguez-Navarro, A. & García-Ruiz, J. M. 2000 Model of textural development of layered aggregates. *Eur. J. Mineral.* **12**, 609–614.

Saleuddin, A. S. M. & Kunigelis, S. C. 1984 Neuroendocrine control mechanisms in shell formation. *Am. Zool*. **24**, 911–916.

Schaffer, T. E. (and 11 others) 1997 Does abalone nacre form by heteroepitaxial nucleation or by growth through mineral bridges? *Chem. Mater.* **9**, 1731–1740.

Silyn-Roberts, H. & Sharp, R. M. 1986 Crystal growth and the role of the organic network in eggshell biomineralization. *Proc. R. Soc. Lond.* B **227**, 303–324.

Simkiss, K. & Wilbur, K. M. 1989 *Biomineralization: cell biology and mineral deposition*. San Diego, CA: Academic Press.

Sunagawa, I. 1987 *Morphology of crystals*, pp. 511–581. Tokyo: Terra Scientific Publishing Co.

Taylor, J. D., Kennedy, W. J. & Hall, A. 1969 The shell structure and mineralogy of the Bivalvia. Introduction. Nuculacea–Trigonacea. *Bull. Br. Mus. Nat. Hist. Zool*. **3**(Suppl.), 1–125.

Ubukata, T. 1994 Architectural constraints on the morphogenesis of prismatic structure in Bivalvia. *Palaeontology* **37**, 241–261.

Weiner, S. & Traub, W. 1980 X-ray diffraction study of the insoluble organic matrix of mollusk shells. *FEBS Lett*. **111**, 311–316.

Weiner, S. & Traub, W. 1984 Macromolecules in mollusc shells and their functions in biomineralization. *Phil. Trans. R. Soc. Lond.* B **304**2, 425–435.

As this paper exceeds the maximum length normally permitted, the authors have agreed to contribute to production costs.